

A Miniature Hybrid Robot Propelled by Legs

Matthew C. Birch, Roger D. Quinn, Geon Hahm, Stephen M. Phillips, Barry Drennan, Andrew Fife, Randall D. Beer, Xinyu Yu, Steven L. Garverick, Sathaporn Laksanacharoen, Alan J. Pollack, Roy E. Ritzmann

Case Western Reserve University
Cleveland, Ohio 44106

Abstract

This paper describes the development of an autonomous hybrid micro-robot that uses legs for propulsion and support of the rear half of the body and uses a pair of wheels for support of the front half. McKibben artificial muscles actuate the legs and the compressed air that activates the actuators is generated by an on-board power plant made up of a pair of lithium batteries powering a gear motor driven air compressor. The control is also onboard in the form of a PIC that controls the actuators through four three-way valves that each consists of a pair of MEMS devices.

1. Introduction

The Biorobotics group at CWRU has been building biologically inspired robots for the last eleven years. The team on this project includes mechanical and electrical engineers, computer scientists, and biologists. We have gained valuable insight into the biological systems modeled. The biologists have used the engineering research to help evaluate their findings. We have built three generations of robots using biological principles. Robot I demonstrated the flexibility of a neural network controller [20]. Robot II's controller incorporated reflexes observed in insects. This made it able to deal with rough terrain and obstacles [11]. Robot III, still in development, is a pneumatically actuated robot modeled closely after a cockroach and has so far been shown to have exceptional power, robust posture control, and smooth motor motion and promises to be an agile robot [3], [17], [18]. With our experience in design and construction of insect inspired robots we have miniaturized what we have learned to make a microrobot based loosely upon cricket locomotion.

In this paper we describe an autonomous hybrid microrobot (Figure 1). By hybrid we mean that it uses both wheels and legs. The small size requirement was the greatest challenge of the project due to the manufacturing and assembly of components. Developing a small, light, power source was particularly challenging. The hybrid robot uses its legs as the drive mechanism and its passive wheels have a large diameter to help the robot propel itself over obstacles. This hybrid design allows for more capable locomotion than a design using all wheels, and yet provides a simpler system than a totally legged robot. Two lithium batteries power a Smoovy™ motor that

drives a compressor that, in turn, supplies air for the leg actuators. A rule-based controller switches an array of

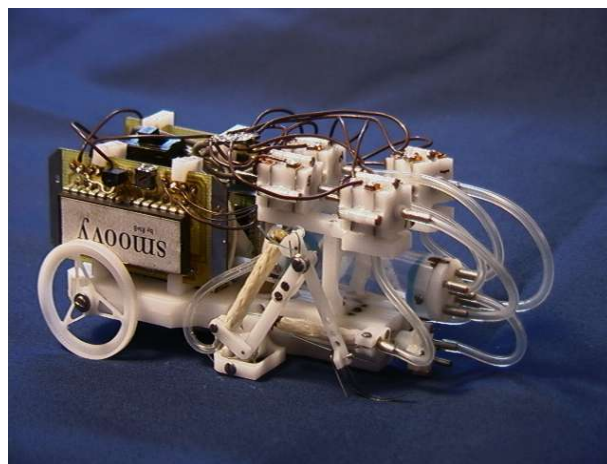


Figure 1. The hybrid robot uses its rear legs for propulsion and its front wheel help to support the body weight.

two-way MEMS valves that distribute the compressed air to the actuators.

2. Cricket Biology

The legged propulsion of the hybrid robot was inspired by the locomotor behavior of the house cricket, *Acheta domestica*. Insects have three pairs of legs, and have evolved highly efficient segmental construction and actuation to optimize their specialized locomotory behaviors. The cricket has large and powerful rear legs that enable fast, long jumps as well as stable, reciprocating walking (Fig 2A, Leg Schematic) [14].

As a design input for the robot legs, we studied the movements of cricket hind legs while the animal was walking and jumping. These were viewed in a transparent, Plexiglass™ treadmill with a clear acetate belt. We used a high-speed digital video system (Redlake PCI 500, at 250fps) to record movement. High-contrast dots were painted on the ends of the major segments (Fig. 2B-C) to enable spatial representation. A side view and a bottom (ventral) view were combined to provide x, y, and z space coordinates. These points were then converted into three-dimensional data on joint angle positions, which were incorporated into a dynamic model. Simulations

were the legs.

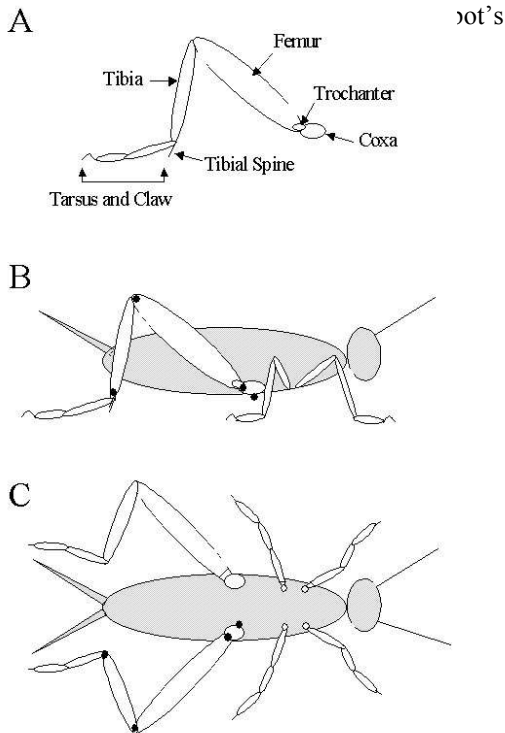


Figure 2. Cricket configuration. A) Leg segments. B) Side view. C) Ventral view.

The leg movements during walking employ a tripod gait, which is the standard for insect locomotion. Because of the large powerful rear legs, the joint movements of the cricket varied somewhat from patterns seen in cockroach [23]. The orientation of the cricket hind leg is more vertical than that of the cockroach. Joint movement patterns are similar, though, in that the propulsive phase (stance) of the leg is characterized by a synchronous increase in the coxa-trochanter-femur and femur-tibia (Fig 2A) joint angles. These excursions extend the femur back and drive the tibia downward and to the rear, resulting in forward movement of the body. A swing phase follows,

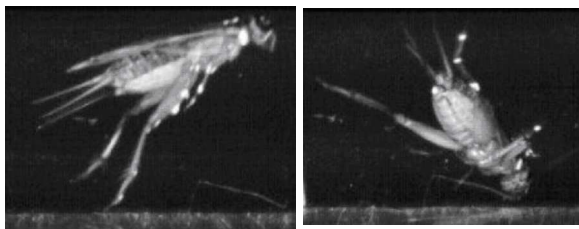


Figure 3. a) Cricket jumping with its tarsal spines intact. b) Unsuccessful jumping with its spines removed.

during which each leg of a tripod is brought up and forward in preparation for the next cycle.

In jumping, the cricket cocks its legs and then rapidly extends them downward, driving the animal up into a long arched jump trajectory. We identified three spines at the base of the tibia (Fig 2A) that are critical to a successful jump. They grip the substrate providing a stop for the powerful leg movements. Figure 3A shows a thrusting takeoff in an animal with these spines intact. Removing these spines compromises the jump and the animal merely pitches over and lands on its head immediately right in front of the jump site (Fig 3B). The importance of these spines and their passive nature inspired us to incorporate similar structures on the legs of the robot (Fig 4).

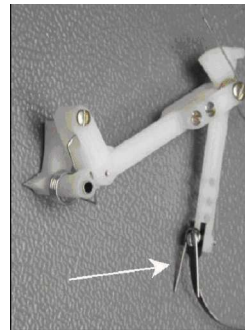


Figure 4. One leg of the hybrid robot with torsional return springs and spines

3. Cricket Simulation

The walking behavior of the cricket was incorporated into a dynamic simulation with 6 degrees of freedom (DOF) for the body (three translations and three rotations), which is assumed rigid, and 5 DOF for each of the cricket's 6 legs. The body-coxa joint, the coxa-trochanter-femur joint, and the femur-tibia joint are modeled with 3, 1 and 1 DOF, respectively [Noom ICRA xx].

Inputs to the dynamic simulation include the joint angle trajectories and the inertia of all the leg segments and the body. Outputs include joint torques, body movements, ground reaction forces, and moments in the leg segments. A proportional plus derivative control law is used in the simulation to cause the model's joints to follow the measured cricket joint data [6].

Joint torques are not measured directly in the live cricket, so their simulation was essential in power source selection. Ground reactions provided information on leg strength and material requirements and were similar to results obtained in other insect preparations [12] and simulation [16].

4. Hybrid Robot Simulation

For modeling, design and control purposes a faster dynamic simulation of the hybrid robot was developed. The starting point was the cricket model, but it was simplified to be a planar system with just two legs based on the cricket's rear legs. This simulation was used to understand the displacements and forces for the robot, to refine the robot design and to evolve a controller as described in Section 10.

The robot model has two two-segment legs which attach to the body at its center of mass. Each joint is extended by a modeled McKibben actuator [8], and is flexed by a passive linear spring. The model was formulated using Lagrange's equations and it is numerically integrated using the fourth-order Runge-Kutta method to perform a simulation. The inputs from a controller are signals that open and close the modeled MEMS valves. The outputs include joint and body motions and ground reaction forces.

5. Robot Design

The hybrid cricket robot is propelled by a pair of two DOF rear legs based on the rear legs of the cricket. In this hybrid robot design, the front two pairs of legs have been replaced with a single pair of wheels. This was done to keep the number of valves and flow rate of compressed air to a minimum.

Most of the structure of the robot is made from Delrin using a desktop CNC milling machine. Since this is a prototype robot much of it is made to be assembled and disassembled repeatedly. Therefore, much of the robot is assembled with sixty 00-90 screws and about fifteen 0-80 screws. The robots will ultimately be use-and-discard devices that will be mass-produced.

The legs have two DOF that are actuated with a spring-actuator antagonist pair. The actuated joints in the robot are constructed of Delrin bushings on stainless steel tubular axles. This combination of materials gives a low friction, dry bearing. The tarsus (foot) of the robot is constructed of 0.005-inch thick spring steel with 0.150-inch thick music wire to make the spines (Fig. 4). The arrangement provides a compliant foot that gives good traction on rough and most smooth surfaces.

The chassis is one piece and made of Delrin. The compressor is mounted in the back half of the chassis along the centerline. The crank and rocker mechanism along with the piston of the compressor is underneath the robot and is protected by a removable cover. The motor rises between the body-femur joints of the legs in the middle of the chassis. The origins of the body-femur actuators are at the posterior end of the chassis on either side. Just above the actuators and compressor mechanism is the pressure reservoir. The MEMS valves are mounted just above the reservoir to minimize the amount of tubing. The front of the chassis has the wheels on the outboard sides with the batteries down the center and with one battery stacked on top of the other. Mounted on both sides of the batteries are the racks that support the two circuit boards. The robot weighs 94 grams. Its wire and hoses, circuit boards, and batteries weigh 22 grams, 30

grams, and 28 grams, respectively. Thus, the chassis, compressor, actuators and legs weigh less than 20 grams.

6. Actuators

The hybrid microrobot uses braided pneumatic actuators to extend the leg segments [6]. These actuators, also known as McKibben artificial muscles, have gross properties similar to muscle [2][10]. Each moveable leg segment retracts by an antagonistic torsion spring.

Braided pneumatic actuators are composed of an expandable bladder surrounded by an inelastic tubular mesh (Fig. 5). When the bladder is inflated, the increase in volume causes the mesh to expand in diameter and contract along its length. The actuators for the hybrid microrobot are very small (1.125" long and 0.125" O.D. when deflated) and while they are not commercially available, they can be mass-produced.

The inner bladder for the actuators is made from high-grade liquid latex. Stainless steel wire (0.064 inch O.D., six inch length) is used as the mold. The wire is first



Figure 5. This side view of the rear half of the robot shows a leg with its two McKibben artificial muscles and the motor that drives the

dipped in a proprietary wetting solution, provided by Kent Elastomer Products, Inc., of Kent, Ohio, followed by latex dipping, drying and leaching.

Tubes are then sent to Fiber Architects, Inc., of Philadelphia, PA for the addition of the braided mesh. This mesh is woven from sixteen bundles of micro-deiner polyester fiber. Eight bundles are wound clockwise and the other eight counter clockwise. The starting angle for the uninflated weave was set to be between 20 and 25 degrees. This is a workable compromise between a smaller initial angle providing for greater contraction during inflation and a larger initial angle providing better mesh stability.

The actuators are cut to the desired 1.125 inch length and a small (0.125 inch length, 0.050 inch O.D.) section of hollow stainless tubing is wire-crimped to one end. This provides the air inlet / outlet via a flexible polyethylene tube, and is clamped to the leg at the actuator's origin. The other end has a short length of 0.020 inch nylon monofilament line as the tendon which attaches the actuator to the anchor point on the adjacent active leg segment.

7. Compressor

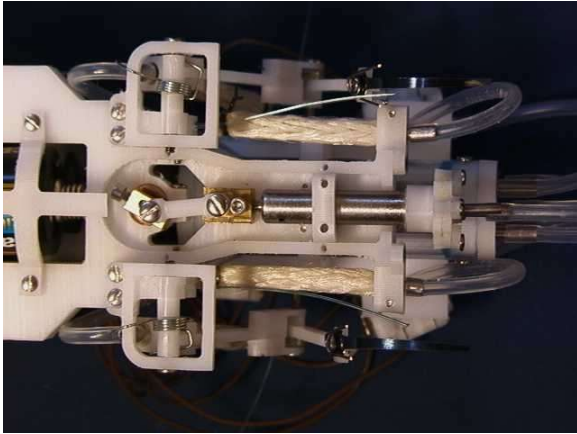


Figure 6. This bottom view of the hybrid robot with the compressor cover removed shows the compressor integrated into the rear half of the chassis.

An on-board air compressor powers the braided pneumatic actuators [6]. A motor with a transmission drives a crank and rocker mechanism that reciprocates a piston in a cylinder (Figures 5, 6 and 7). The first version of the compressor uses Smoovy's standard five-millimeter gear motor with a transmission ratio of 25:1. The Smoovy™ gear motor has a three-pole brush-less stepper motor with a multi stage planetary transmission. The motor runs at 15000 RPM, which results in a 10Hz reciprocation of the piston. Because of torque limitations of the five-millimeter motor the first compressor used a 0.080-inch crank arm. The resulting 0.160 inch stroke produces the lower line in Figure 8 which is a plot of pressure vs. flow for the compressor. This was below the needed 0.09 Liters/min. at 7 psi that was calculated to be the minimum requirement to run the robot. Smoovy recently provided an eight-millimeter motor with a prototype adapter for the existing five-millimeter transmission. The resulting gear motor has a final transmission ratio of 25:1. With this new motor we were able to greatly lengthen the crank arm thus lengthening the stroke. The other three lines in Figure 8 show progressively more flow and correspond to increasing lengths of the crank while using the eight-millimeter motor.

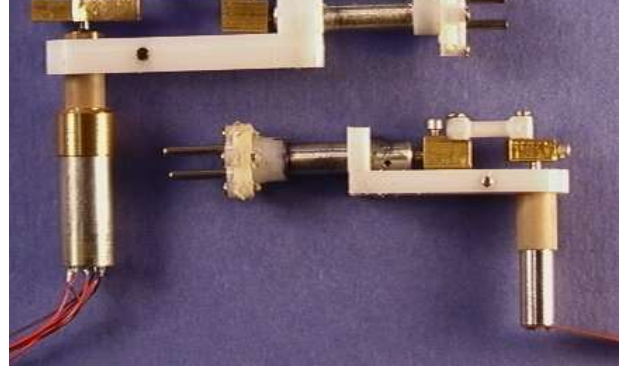


Figure 7. The original compressor that uses a 5mm motor is on the right and the new compressor that uses an 8mm motor is on the left.

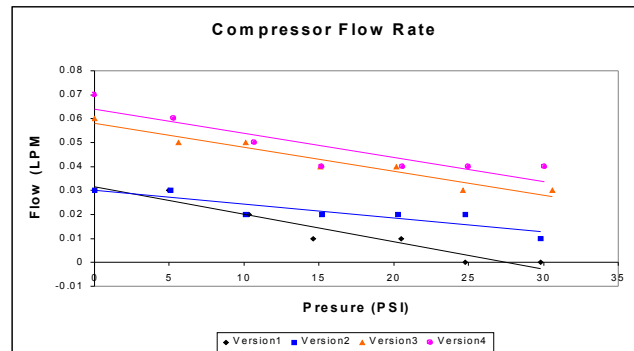


Figure 8. Flow rate versus pressure for four compressors.

The axles are made from stainless steel tubing with Delrin bushings. The crank and rod-end are machined from brass. The piston and cylinder wall is a modification of a 5/32 bore one-inch stroke air cylinder. The piston used in the Clippard cylinder has a Viton cupped O-ring seal on a brass piston with a stainless steel shaft and a return compression spring in the cylinder. The cylinder is stainless steel with a bore of 5/32 and a wall thickness of about 0.015 inches. The spring in the cylinder helps smooth the torque-curve necessary to drive the compressor through one cycle.

The check valves are made with a machined Delrin package that encloses a pair of very small latex flapper valves. The flaps created a pair of check valves arranged so that one is an inlet and the other the outlet. This was accomplished while putting the valves within 0.010 inches of the top of the piston and keeping all the porting within the confines of the 5/32 bore cross-section. The compressor was designed to operate at 35 psi but has reached nearly 50 psi in testing.

8. MEMS SMA Valves

Each valve consists of a flat silicon spring, a co-sputtered and patterned Titanium-Nickel (TiNi) shape memory alloy (SMA) actuator, and an orifice. All three components are batch micro-fabricated using silicon substrates.

Figure
Fig

A TiNi SMA actuator has been chosen because its high strains (3%) [13] and actuation forces (work density of $5 \times 10^6 \text{ J/m}^3$) enable high fluid flow rates and high working pressures, respectively. The transformation temperatures and strains are very sensitive to compositional variation. Since the Ti and Ni constituents in alloy sputtering targets have different sputtering yields during deposition, a co-sputtering procedure has been developed which uses an alloy TiNi target and an elemental Ti target to reliably achieve stoichiometric SMA films [21].

The valve is normally closed; the fluid flow is proportional to the current applied. The patterned TiNi actuator and silicon spring allow “flow-through” operation. The spring provides an initial closing force against the orifice making the valve normally closed when the SMA actuator is in its low temperature martensite phase (Figure 9a). When the actuator is heated, it transforms to austenite, forcing the spring upward, opening the valve (Figure 9b). The orifice die simply contains a square inlet.

Three types of valve packages have been developed. Two

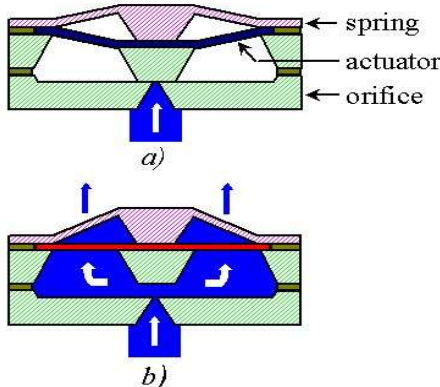


Figure 9. Cross-section of a microvalve. a) closed position, b) open position

Figure 9. Cross-section of a microvalve. a) closed position. b) open position

of them are for completed devices, which are two-way and three-way valves. The other is for testing device components. Figure 10 shows a 3-way micro-valve and a test package. This packaging scheme allows reliable and repeatable testing of device components.

Flow rates of up to 0.5 Liters/min are achieved for an input air pressure of 245 kPa and the leakage is less than 0.005 lpm. The micro-valve is actuated with 100 mA and the power consumption is 370 mW. The time response of the micro-valve controlled pneumatic actuators was acquired using digital video recording. The on time is about 100 msec and the off time is about 150 msec. The

fatigue of TiNi SMA actuator is less than 5% after over 1 million cycles of actuation.

9. On Board Electronics

On-board electronics consist of two parts: controller hardware and power source. A PIC micro-controller operates the voltage regulator and the MEMS valves as shown in Figure 11.

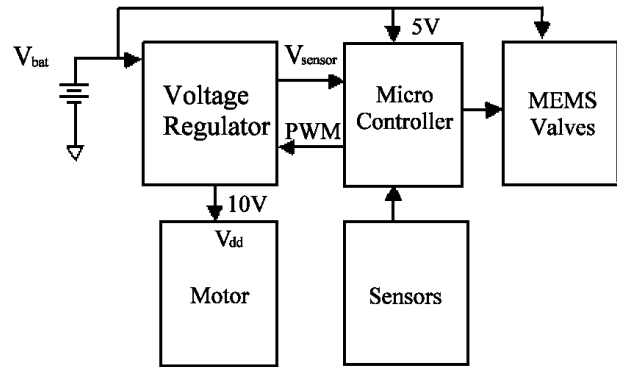


Figure 11. Block Diagram of on board electronics

The power source for the robot is a pair of CR-2 3V lithium batteries, which can run the robot for about 20 min. The motor operates best at 10 Volts, for which it drains about 160 mA current. Each MEMS valve draws 100 mA current at 5 Volts when it is on. In this application, four valves can be on at the same time. As a result, the maximum power consumed by the robot is about 3.6 Watts.

A switching voltage regulator is used to convert the 5V battery voltage to 10 Volts [1]. Figure 12 is the schematic of the voltage regulator. The basic operation of this circuit consists of two parts corresponding to the level of gate voltage V_g of transistor M1. When V_g is high, M1 is on, the diode D1 is reverse-biased, and energy is stored in the inductor. When V_g goes low, M1 is off, D1 is forward biased, and the energy stored in the inductor is transferred to the capacitor. The capacitor charges until the energy balance is reached. V_g is controlled by a Pulse Width Modulation (PWM) signal, whose duty factor can be changed.

The result of an open-loop simulation shows that output voltage (V_{out}) has a linear relationship with the duty factor of the PWM input (DF) for $DF < 67\%$. The gain factor is 10–22 V/DF depending on the number of valves opened. Power efficiency is 87% - 92%, if DF is less than 67%.

Based on the open-loop result, a close-loop control algorithm has been designed to maintain V_{out} at a desired value. The microcontroller senses V_{out} via its A/D

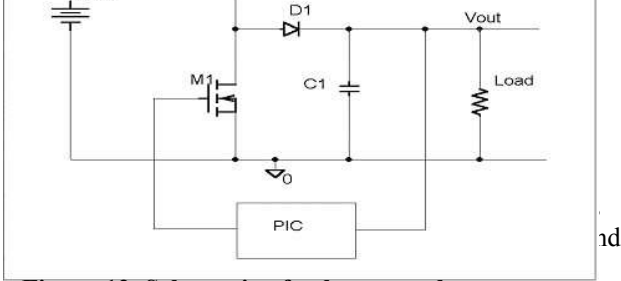


Figure 12. Schematic of voltage regulator. When the input voltage is high, the PIC reduces the duty factor of the PWM output, and vice versa.

10. Controller

Two controllers were developed for the robot: a feed-forward scheme using timing, and a feedback scheme using a continuous-time recurrent neural network (CTRNN) in the control loop. The feed-forward controller, programmed on a PIC microcontroller, sends a sequence of pulses to the actuator valves to operate the legs. It ignores feedback signals completely, and depends on the legs reaching their extents of motion to maintain its operating range over time.

The CTRNN-based controller was developed using a genetic algorithm (GA) operating on a simplified robot simulation to search the multidimensional neuron parameter space – in this case, 61 dimensions. In earlier work, the fitness function was trajectory-based, minimizing the mean-square error from a predetermined joint angle trajectory [6]. However, a behavior-based function, wherein a general global behavior is measured and rewarded or penalized, is a more efficient method of measuring fitness. The fitness function used in this search was the forward progress of the robot at the end of its 10-second trial.

A real-valued genetic algorithm [22] was used to evolve CTRNN parameters. A population included individuals encoded as a length M vector of real numbers. Initially, a random population of vectors was generated. Individuals were selected for reproduction using a linear rank-based method. A specified elitist fraction of top individuals in the old population were simply copied to the new one. The remaining children were generated by either mutation or crossover with an adjustable crossover probability. A neuron's time constant, bias, and output weights were treated as a module during crossover. The search parameters in the range ± 1 were mapped linearly into CTRNN parameters with the following ranges: connection weights $\in [-8, 8]$, biases $\in [-4, 4]$, and time constants $\in [0.01, 0.1]$. All neuron gains were set to unity.

The neural net architecture (see Figure 13) consists of sixteen symmetrically arranged neurons. The input neuron layer has feed-forward connections to the layer of "interneurons" which consists of three neurons on each side, and whose neurons are fully interconnected with each other and themselves. The three interneurons on each side have feed forward connections to the output layer of neurons. Each neuron – two per side – controls the valves for one actuator. Thresholds were evolved to

determine what levels would indicate valve openings and closings.

11. Neural Network & Controller Hardware

The robot used a Microchip PIC 18C252 microcontroller

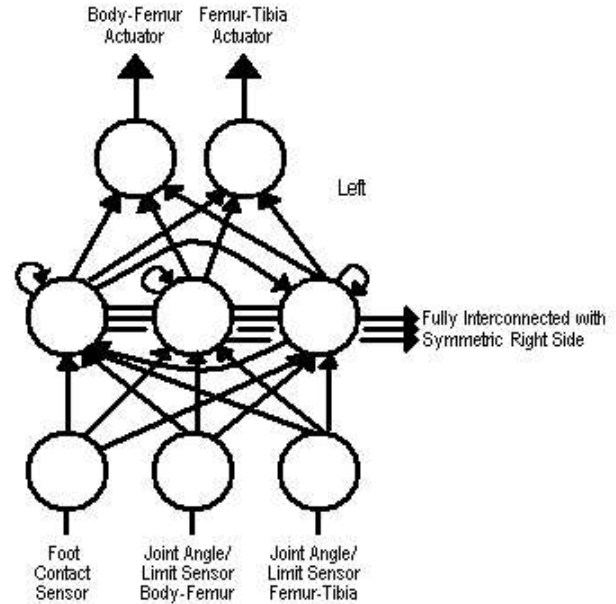


Figure 13. Fully connected, continuous time recurrent neural network for control of locomotion.

All of the components for the hybrid robot described above were shown to work independently. Next, the hybrid robot was assembled using those components and all of them were shown to be operational on-board the robot. However, while the original compressor was operational, it did not supply sufficient airflow to the robot to activate the actuators. Therefore, the robot was demonstrated to walk using an external air supply. As discussed in the compressor section above, the compressor has since been greatly improved.

A purely legged robot is also being developed using the hybrid robot's components [6]. A conceptual design of this robot is shown in Figure 14. This robot will also be autonomous and locomote by walking and jumping. It should be capable of climbing over larger obstacles using its front legs. The front legs will also be used to control the pitch of the body before a jump and, therefore, aim the jump for distance or height.

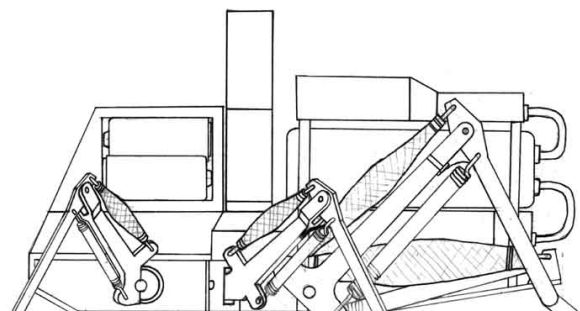


Figure 14. Conceptual design of a legged micro-robot that can walk and jump

This work was supported by the DARPA Distributed Robotics Program under contract DARPA/ETO DAAN02-98-C-4027. We would also like to thank Chris Pastore at the Philadelphia College of Textile and Science for braiding our pneumatic actuators.

References

1. Abraham I. Pressman, *Switching Power Supply Design*, 2nd edition. New York : McGraw-Hill, c1998.
2. Alexander, R. McN. (1988). *Elastic Mechanisms in Animal Movement*. Cambridge University Press, NY
3. Bachmann, R.J., Nelson, G.M., Flannigan, W.C., Quinn, R.D., Watson, J.T., Ritzmann, R.E., (1997). "Construction of a Cockroach-like Hexapod Robot." Proc. of the 11th VPI&SU/AIAA Symp. on Dyn. and Cont. of Large Structures, Blacksburg, VA.
4. Beer, R.D. (1995). On the dynamics of small continuous-time recurrent neural networks. *Adaptive Behavior* 3(4):471-511.
5. Beer, R.D., Quinn, R.D., Chiel, H.J., Ritzmann, R.E., (1997). "Biologically-Inspired Approaches to Robotics." *Communications of the ACM*, Vol. 40, No. 3.
6. Birch, M.C., Quinn, R.D., Hahm, G., Phillips, S., Drennan, B., Fife, A., Verma, H., Beer, R.D. (2000). "Design of a cricket microrobot," IEEE Conf. on Robotics and Automation, April 2000, San Francisco, CA.
7. Brown, B., Garverick, S. L. 1999, "Analog VLSI implementation of a neural network controller" MS Thesis at Case Western Reserve University
8. Colbrunn, R. (2000). Design and Control of a Robotic Leg with Braided Pneumatic Actuators, M.S. Thesis, Case Western Reserve University, Cleveland, Ohio.
9. Caldwell, D. G., Medrano-Cerda, G. A., and Bowler, C. J., "Investigation of Bipedal Robots Locomotion Using Pneumatic Muscle Actuators" proceedings of the 1997 IEEE international Conference on Robotics and Automation, Albuquerque, NM, 1997
10. Chou, C., Hannaford, B., "Measurement and Modeling of McKibben Pneumatic Artificial Muscles" IEEE transactions on Robotics and Automation Vol. 12, No. 1, February 1996
11. Espenschied, K.S., Quinn, R.D., Chiel, H.J., Beer, R.D. (1996). "Biologically-Based Distributed Control and Local Reflexes Improve Rough Terrain Locomotion in a Hexapod Robot". *Robotics and Autonomous Systems*, Vol. 18, 59-64.
12. Full, R.J. (1993). Integration of Individual Leg Dynamics with Whole Body Movement in Arthropod Locomotion. *Biological Neural Networks in Invertebrate Neuroethology and Robotics*, Academic Press, NY.
13. Krulevitch, P.; Lee, A.P.; Ramsey, P.B.; Trevino, J.C.; Hamilton, J.; Northrup, M.A., "Thin Film Shape Memory Alloy Microactuators," *J. MEMS*, 5 [4] (1996) 270-282.
14. Laksanacharoen, S., Pollack, A., Nelson, G.M., Ritzmann, R.E., Quinn, R.D. (2000). "Biomechanics and simulation of cricket for microrobot design," IEEE Conf. on Robotics and Automation, April 2000, San Francisco, CA.
15. Mitchell, M. (1996) *An Introduction to Genetic Algorithms*, MIT Press.
16. Nelson, G. M. and Quinn, R. D. (1995) "A Lagrangian Formulation in Terms of Quasicoordinates for Dynamic Simulations of Multibody Systems such as Insects and Robots," 1995 ASME International Mechanical Engineering Congress and Exposition (IMECE 1995), San Francisco, California.
17. Nelson, G. M. and Quinn, R. D. (1998). "Posture Control of a Cockroach-like Robot." IEEE International Conference on Robotics and Automation (ICRA'98), Leuven, Belgium.
18. Nelson, G.M., Bachmann, R.J., Quinn, R.D., Watson, J.T., Ritzmann, R.E., (1998). "Posture Control of a Cockroach-like Robot (Video)". Video Proc. Of the IEEE Int. Conf. on Robot. and Automat. (ICRA '98), Leuven, Belgium.
19. Pratt, J., Dilworth, P., Pratt, G., (1997). "Virtual Model Control of a Bipedal Walking Robot." Proc. of the IEEE Int. Conf. on Robot. and Automat. (ICRA 97), Albuquerque, NM.
20. Quinn, R. D. and Espenschied, K. S., (1992). Control of a Hexapod Robot Using a Biologically Inspired Neural Network. *Biological Neural Networks in Invertebrate Neuroethology and Robotics*, Academic Press.
21. Shih, C.L.; Lai, B.K.; Kahn, H.; Phillips, S.M.; Heuer, A.H., "A Robust Co-Sputtering Fabrication Procedure for TiNi Shape Memory Alloys for MEMS," *J. MEMS*, (2000)
22. Slocum, A.C., Downey, D.C. and Beer, R.D. (2000). Further experiments in the evolution of minimally cognitive behavior: From perceiving affordances to selective attention. In J. Meyer, A. Berthoz, D. Floreano, H. Roitblat and S. Wilson (Eds.), *From Animals to Animats 6: Proceedings of the Sixth International Conference on the Simulation of Adaptive Behavior* (pp. 430-439). MIT Press.
23. Watson, J.T. and R.E. Ritzmann (1998) Leg kinematics and muscle activity during treadmill running in the cockroach, *Blaberus discoidalis*: I. Slow running. *J. Comp. Physiol A*. 182:11-22.